Cancer Pathogenesis and Therapy 1 (2023) 18–24

Contents lists available at ScienceDirect

Cancer Pathogenesis and Therapy

journal homepage: www.journals.elsevier.com/cancer-pathogenesis-and-therapy

Research article

Prognostic biomarkers and immune cell infiltration characteristics in small cell lung cancer

Jun Ni, Xiaoyan Si, Hanping Wang, Xiaotong Zhang, Li Zhang *

Department of Pulmonary and Critical Care Medicine, Peking Union Medical College Hospital, Chinese Academy of Medical Science & Peking Union Medical College, Beijing 100730, China

HIGHLIGHTS

- Gene prostaglandin-endoperoxide synthase 2 (*PTGS2*) is a potential prognostic biomarker of small cell lung cancer (SCLC).
- Resting memory $CD4^+$ T cells might be the predominant infiltrating immune cells in SCLC.
- Hub genes and tumor-infiltrating immune cells may be the molecular mechanisms underlying the development of SCLC.

GRAPHICAL ABSTRACT

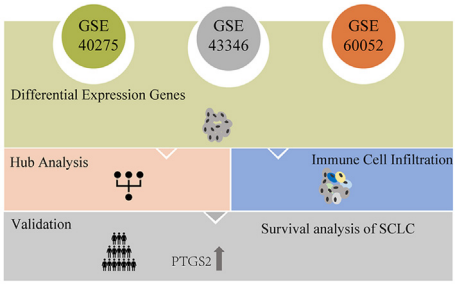

A total of 312 robust differentially expressed geneswere screened from 129 Small cell lung cancer (SCLC) tissue samples and 44 normal tissue samples obtained from Gene Expression Omnibus. Kaplan–Meier plotter revealed that the gene prostaglandin-endoperoxide synthase 2 (*PTGS2*) was a potential prognostic biomarker for SCLC.

ARTICLE INFO

Keywords:
Bioinformatics analysis
Small cell lung cancer
Immune cell infiltration
Tumor microenvironment
Hub genes
Protein interaction network
Gene expression omnibus database

ABSTRACT

Background: Small cell lung cancer (SCLC) is a highly malignant and aggressive neuroendocrine tumor. With the rise of immunotherapy, it has provided a new direction for SCLC. However, due to the lack of prognostic biomarkers, the median overall survival of SCLC is still to be improved. This study aimed to explore novel biomarkers and tumor-infiltrating immune cell characteristics that may serve as potential diagnostic and prognostic markers in SCLC.
Methods: Gene expression profiles from patients with SCLC were downloaded from the Gene Expression Omnibus (GEO) database, and tumor microenvironment (TME) infiltration profile data were obtained using CIBERSORT. The robust rank aggregation (RRA) method was utilized to integrate three SCLC microarray datasets downloaded from the GEO database and identify robust differentially expressed genes (DEGs) between normal and tumor tissue samples. Gene Ontology (GO) and Kyoto Encyclopedia of Genes and Genomes (KEGG) enrichment analyses were performed to explore the functions of the robust DEGs. Subsequently, protein–protein interaction networks and key modules were constructed by Cytoscape, and hub genes were selected from the whole network using the plugin cytoHubba. Survival analysis of hub genes was performed by Kaplan–Meier plotter in 18 patients with extensive-stage SCLC.
Results: A total of 312 robust DEGs, including 55 upregulated and 257 downregulated genes, were screened from 129 SCLC tissue samples and 44 normal tissue samples. GO and KEGG enrichment analyses revealed that the robust DEGs were predominantly involved in human T-cell leukemia virus 1 infection, focal adhesion, complement and coagulation cascades, tumor necrosis factor (TNF) signaling pathway, and ECM-receptor interaction, which are closely associated with the development and progression of SCLC. Subsequently, three DEGs modules and six hub genes (*ITGA10*, *DUSP12*, *PTGS2*, *FOS*, *TGFBR2*, and *ICAM1*) were identified through screening with

* Corresponding author. Department of Pulmonary and Critical Care Medicine, Peking Union Medical College Hospital, Chinese Academy of Medical Science & Peking Union Medical College, Beijing 100730, China
E-mail address: zhanglipumch1026@sina.com (L. Zhang).

https://doi.org/10.1016/j.cpt.2022.09.004
Received 21 July 2022; Received in revised form 10 September 2022; Accepted 26 September 2022
2949-7132/© 2022 Published by Elsevier B.V. on behalf of Chinese Medical Association (CMA). This is an open access article under the CC BY-NC-ND license (http://creativecommons.org/licenses/by-nc-nd/4.0/).

the Cytoscape plugins MCODE and cytoHubba, respectively. Immune cell infiltration analysis by the CIBERSORT algorithm revealed that resting memory $CD4^+$ T cells were the predominant infiltrating immune cells in SCLC. In addition, Kaplan–Meier plotter revealed that the gene prostaglandin-endoperoxide synthase 2 (*PTGS2*) was a potential prognostic biomarker of SCLC.
Conclusions: Hub genes and tumor-infiltrating immune cells may be the molecular mechanisms underlying the development of SCLC, and this finding could contribute to the formulation of individualized immunotherapy strategies for SCLC.

Introduction

Small cell lung cancer (SCLC) is a highly malignant and aggressive neuroendocrine tumor characterized by rapid growth and early metastasis, and accounts for approximately 10–15% of lung cancers.[1,2] Platinum-etoposide chemotherapy is the first-line treatment for SCLC, but most patients experience drug resistance or disease recurrence. Median overall survival in extensive SCLC is approximately 8–10 months, with a 2-year survival rate of only 8% and a 5-year survival rate of <1%.[3,4] Immune checkpoint inhibitors combined with chemotherapy improved the median overall survival (OS) in SCLC to 12.3–13 months,[5,6] a milestone event in the treatment of SCLC.

The molecular basis of SCLC development is relatively complex and involves various molecular biological events such as chromosome instability, oncogene activation, tumor suppressor gene inactivation, disorder of molecular signaling systems, and loss of DNA mismatch repair function.[7] The most common gene mutations in SCLC are double allele inactivation of tumor suppressor genes Tumor Protein 53 (*TP53*) and RetinoBlastoma 1 (*RB1*), increased copy number of myelocytomatosis (*MYC*) family members, and alterations in enzymes and kinase signaling pathways involved in chromatin remodeling.[8] However, there are currently limited targeted agents with significant antitumor activity in SCLC.[9] To improve the efficacy of SCLC therapeutics, it is essential to elucidate genomic changes in SCLC, understand SCLC at the molecular level, and identify biomarkers associated with prognosis. Immune escape mechanisms are crucial in the development and progression of SCLC. Immune checkpoint inhibitors have produced significant and durable clinical effects in approximately 20% of patients with non-small cell lung cancer (NSCLC), and tumor-infiltrating immune cells have been found to serve as prognostic biomarkers.[10,11] Therefore, it is urgent to further explore the molecular mechanisms of SCLC and potential biomarkers for early screening and targeted therapy for SCLC. Gene microarray technology and bioinformatics analyses have been widely used in genomics studies in recent years. However, due to the characteristics of SCLC, relevant gene microarray data are scarce. Rohrbeck et al.[12] analyzed messenger RNA (mRNA) expression in SCLC and found that abnormal expression of genes such as cyclin-dependent kinase (*CDK*), neural cell adhesion molecule 1 (*NCAM1*), and drosophila Eph kinase (*DEK*) was associated with the development of SCLC.

The current study aimed to further explore the molecular mechanisms of SCLC by integrating multiple SCLC gene expression microarray datasets from the public gene microarray database (Gene Expression Omnibus [GEO]), calculating robust differentially expressed genes (DEGs) by bioinformatics, and then performing functional analysis and constructing a protein interaction network, as well as characterizing tumor-infiltrating immune cells.

Methods

Data collection and processing

Gene expression data of SCLC in the GSE40275, GSE43346, and GSE60052 datasets were obtained from GEO (http://www.ncbi.nlm.nih.gov/geo/). Matrix files and platform annotation documents of the three microarray datasets were downloaded. The names of microarray probes were converted to gene symbols by Perl (www.perl.org). DEGs were identified from normal tissue and tumor tissue samples in each dataset using the limma package[13] in R (www.r-project.org) with cutoff criteria of |log fold change (FC)| > 1 and *P*-value < 0.05.

Robust rank aggregation (RRA) analysis

To integrate the three microarray datasets, an RRA approach was employed to screen robust DEGs. Before RRA analysis, up- and down-regulated genes were ranked according to their FC-score in each dataset. Robust DEGs were then obtained based on the ranked genes in the three datasets using the RobustRankAggreg R package.[14] Genes with |logFC| > 1 and *P*-value < 0.05 were considered as the significant robust DEGs.

Functional enrichment analysis

To clarify the underlying biological processes of robust DEGs, Gene Ontology (GO) enrichment results for biological process (BP), cellular component (CC), and molecular function (MF) were obtained using the "clusterProfiler" R package.[15] Kyoto Encyclopedia of Genes and Genomes (KEGG) pathway analysis of robust DEGs was also performed with the "clusterProfiler" R package. *P*-values <0.0001 and < 0.001 for GO and KEGG analyses, respectively, were considered statistically significant.

Construction of protein–protein interaction (PPI) networks and MCODE analysis

Robust DEGs were uploaded to the STRING online database (http://www.string-db.org/) and a confidence level >0.7 was selected as the screening criteria. Visualization of PPI networks was performed using Cytoscape (version 3.8.2, www.cytoscape.org) software, a bioinformatics software platform that enables visualization of molecular interaction networks by building protein interoperability networks. The Cytoscape plugin Molecular Complex Detection Technology (MCODE) was used to screen for significant modules in the PPI networks.

Hub gene identification

The Cytoscape plugin cytoHubba—with algorithms including Degree, Edge Percolated Component (EPC), Maximum Neighborhood Component (MNC), Density of Maximum Neighborhood Component (DMNC), Maximal Clique Centrality (MCC), BottleNeck (BN), EcCentricity, Radiality, Betweenness, and Closeness—was used to predict and explore the SCLC hub genes of tumor tissue samples.

Immune infiltration by CIBERSORT analysis

CIBERSORT[16] is an inverse convolutional integration algorithm for human immune cell subtype expression matrix based on linear support vector regression principles. The algorithm infers the proportion of immune cell types in tumor tissue sample data of mixed cell types. CIBERSORT contains 547 genes, and by relying on highly specific and sensitive gene expression profiles, the algorithm can distinguish 22 human immune cell phenotypes, including B cells (naïve and memory), T cells ($CD8^+$ T cells, naïve $CD4^+$ T cells, resting memory $CD4^+$ T cells, activated memory $CD4^+$ T cells, follicular helper T cells,

regulatory T cells, gamma delta T cells), natural killer (NK) cells (resting and activated), macrophages (M0, M1, and M2), dendritic cells (resting and activated), mast cells (resting and activated), plasma cells, and myeloid subsets (monocytes, eosinophils, neutrophils). Scores for the 22 immune cells were calculated for samples in GSE40275, GSE43346, and GSE60052 datasets based on the CIBERSORT LM22 gene signature, and the immune cell matrix was filtered using a *P*-value <0.05. Relative expression of the 22 immune cells between normal tissue and tumor tissue samples was identified by R package, and principal component analysis (PCA) was also performed.

Survival analysis

The relationship between expression levels of hub genes and prognosis was analyzed using the Kaplan–Meier method in 18 patients with extensive-stage SCLC, and survival curves were plotted.

Results

Identification of DEGs

The SCLC microarray datasets GSE40275, GSE43346, and GSE60052 were collected and analyzed using the limma package in R. The GSE40275 dataset contains 14 normal tissue samples and 8 SCLC tumor tissue samples, calculated on Affymetrix microarrays (Human Exon 1.0 ST Array). The GSE43346 dataset contains 23 normal tissue samples and 42 SCLC tumor tissue samples, detected on the Affymetrix Human Genome U133 Plus 2.0 Array platform. The GSE60052 dataset contains seven normal tissue samples and 79 SCLC tumor tissue samples, processed by Illumina HiSeq 2000 sequencing. Thus, the current study comprised 129 SCLC tumor tissue samples and 44 normal tissue samples; the overall workflow is illustrated in Supplementary Figure 1. Using thresholds of FDR <0.05 and |logFC| > 1, it could be ascertained that there were 3991 DEGs in the GSE40275 dataset (1948 downregulated genes and 2043 upregulated genes), 1890 DEGs in the GSE43346 dataset (895 downregulated and 995 upregulated), and 3442 DEGs in the GSE60052 dataset (2263 downregulated and 1178 upregulated) between normal tissue and tumor tissue samples [volcano plots in Figure 1A–C; heatmaps in Figure 1D–F]. PCA in GSE40274, GSE43346, and GSE60052, respectively, showed that tumor tissue samples could be distinguished from normal samples based on the expression levels of DEGs in each dataset [Figure 1G–I]. To reduce bias, the three datasets were integrated by the RRA method and a total of 312 robust DEGs were identified, including 257 downregulated genes and 55 upregulated genes [Figure 1J].

Functional enrichment analysis

The biological functions and pathways of the 312 robust DEGs were determined using the clusterProfiler package in R. A total of 94 GO terms and six KEGG pathways were enriched (*P*-values <0.0001 and < 0.001, respectively). The highest ranked GO terms in BP, CC, and MF were "regulation of inflammatory response," "membrane raft," and "cytokine binding," respectively. The top 10 GO terms are depicted as bar and bubble plots [Figure 2A,C] In KEGG enrichment analysis, the most highly correlated signaling pathway was complement and coagulation cascades [Figure 2B,D].

PPI network construction and module identification

A protein interaction network of the 312 robust DEGs was constructed through the STRING database with a confidence level >0.7 and hiding the disconnected nodes [Figure 3A]. A visualized PPI network was created by Cytoscape [Figure 3B]. In the final network, 194 nodes and

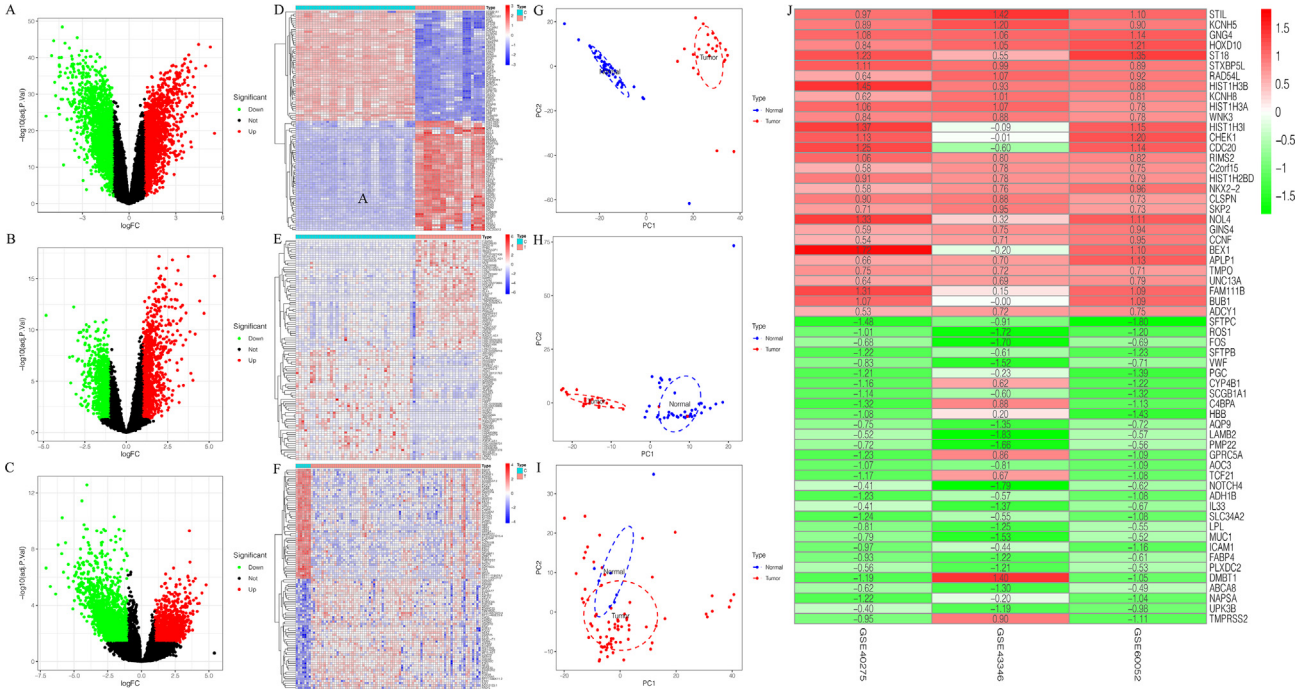

Figure 1. Identification of DEGs and robust DEGs by RRA. (A–C) Volcano plots of the distribution of DEGs in GSE40275 (A), GSE43346 (B), and GSE60052 (C) datasets. The *y*-axis represents the negative log of the *P*-value and the *x*-axis represents the log of FC. Each point represents a gene. Red, green, and black dots denote upregulated DEGs, downregulated DEGs, and non-DEGs, respectively. (D–F) Heatmap plots of the differentially expressed DEGs in GSE40275 (D), GSE43346 (E), and GSE60052 (F) datasets. The horizontal axis represents the samples, the upper horizontal axis represents the sample clusters, the vertical axis represents the DEGs, and the left vertical axis shows the DEGs clusters. Red denotes upregulated genes and green denotes downregulated genes. (G–I) PCA plots of the DEGs in each dataset. The tumor samples (red) and normal samples (blue) are plotted along the axis of the first two principal components (PC1 and PC2). (J) Heatmap of the top 30 upregulated robust DEGs and downregulated robust DEGs identified by RRA. Red represents high expression robust DEGs and green represents low expression robust DEGs. DEGs: Differentially expressed genes; FC: Fold change; PCA: Principal components analysis; RRA: Robust rank aggregation.

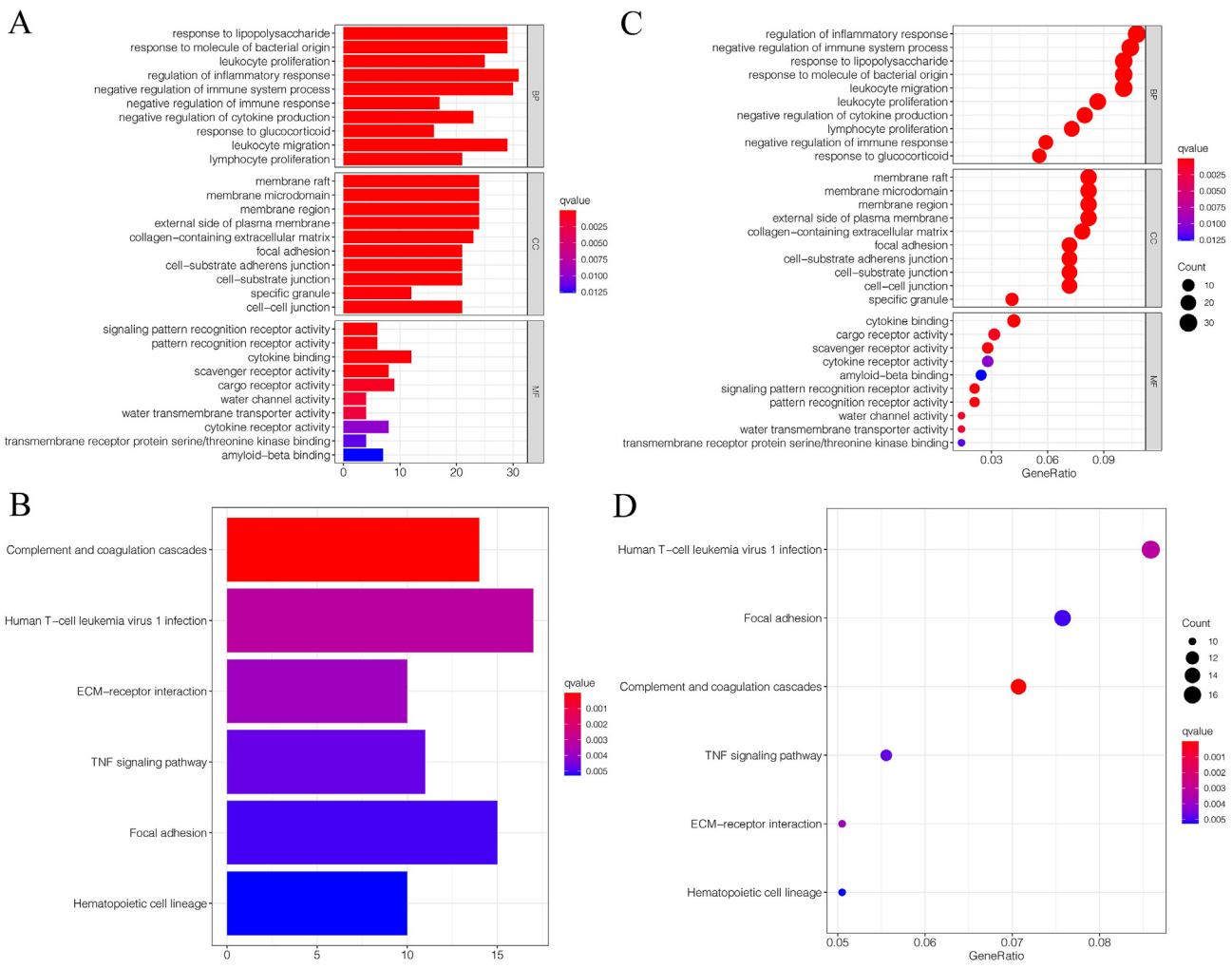

Figure 2. Functional enrichment analysis of robust DEGs. GO enrichment analysis of robust DEGs is visualized in a bar plot (A) and a bubble plot (C). KEGG enrichment analysis of robust DEGs is visualized in a bar plot (B) and a bubble plot (D). DEGs: Differentially expressed genes; GO: Gene Ontology; KEGG: Kyoto Encyclopedia of Genes and Genomes.

325 edges were screened, comprising 155 downregulated genes and 39 upregulated genes. The top three modules were filtered by a score from the whole network by using MCODE, a Cytoscape plugin. The DEGs in Module 1 (score 7) were predominantly enriched in cell cycle and oocyte meiosis pathways, those in Module 2 (score 6) were mainly enriched in extracellular matrix (ECM) -receptor interaction and focal adhesion, and the DEGs in Module 3 (score 4.5) were primarily enriched in tyrosine metabolism.

Identification of hub genes

The top 50 genes of the entire network were selected using the cytoHubba plugin in Cytoscape. The intersection of these 50 genes with 10 algorithms (MCC, DMNC, MNC, Degree, EPC, BottleNeck, EcCentricity, Closeness, Radiality, and Betweenness) identified six hub genes, including integrin alpha 10 (*ITGA10*), dual specificity phosphatase 12 (*DUSP12*), prostaglandin-endoperoxide synthase 2 (*PTGS2*), *FOS*, transforming growth factor beta receptor 2 (*TGFBR2*), and intercellular adhesion molecule-1 (*ICAM1*) [Figure 3C].

Immune cell infiltration analysis

Using the CIBERSORT algorithm, 22 immune cells in tumor tissue and normal tissue samples were evaluated [Figure 4A]. There were significant differences between tumor tissue and normal tissue samples in terms of memory B cells, $CD8^+$ T cells, resting memory $CD4^+$ T cells, resting NK cells, M1 and M2 macrophages, activated dendritic cells, resting mast cells, and neutrophils [Figure 4B and C]. However, PCA showed that immune cell infiltration cannot completely distinguish between SCLC and normal samples [Figure 4D].

Survival analysis

The relationship between the six hub genes and overall survival in 18 patients with extensive-stage SCLC was analyzed using Kaplan–Meier plotter. High expression of *PTGS2* was significantly correlated with longer overall survival (P-value < 0.05) [Figure 5].

Discussion

A high burden of gene mutations and genomic instability of SCLC leads to a high incidence of drug resistance and refractory relapses in patients. *TP53* and *RB1* are the most frequently mutated genes in SCLC,[17] with mutation frequencies of 85% and 57%,[18] respectively, and these mutations are predictors of poor prognosis. The molecular mechanisms underlying the development and progression of SCLC are unclear, and there is an urgent need to identify potential biomarkers of this disease. Bioinformatics can facilitate the exploration of the changes that occur at the genetic level in SCLC, help characterize the tumor microenvironment (TME), and identify potential biomarkers.

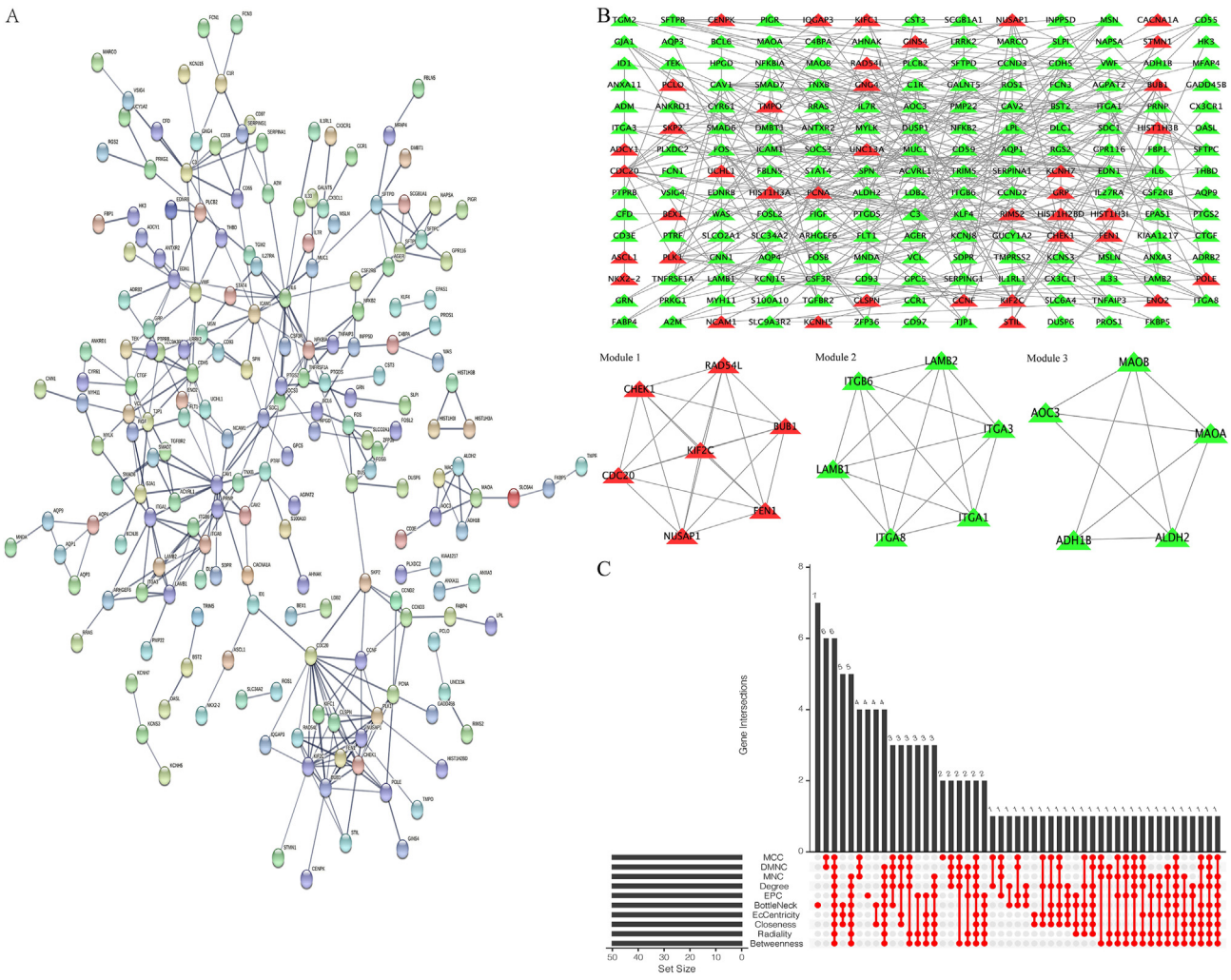

Figure 3. Construction of PPI network, analysis of key modules, and identification of hub genes. (A) Protein interaction network of 312 robust DEGs through the STRING database with a confidence level >0.7 and hiding the disconnected nodes. (B) The whole PPI network. Upregulated robust DEGs are indicated in red, while downregulated robust DEGs are marked in green. (C) Hub genes were selected by the intersection of 50 genes from 10 algorithms. DEGs: Differentially expressed genes; PPI: Protein–protein interaction.

In the present study, three gene microarray datasets – GSE40275, GSE43346, and GSE60052 – were obtained from the GEO database, with each dataset containing a small sample of SCLC tumor tissues. To expand the sample size, explore the mechanisms of SCLC development, and identify tumor-infiltrating immune cells, the three datasets were integrated and then screened for differential genes in SCLC using a bioinformatics approach. This method yielded 312 DEGs, including 257 downregulated genes and 55 upregulated genes. These genes were mainly enriched in GO-BP terms involved in pathways of inflammatory factor secretion, including "response to molecule of bacterial origin," "leukocyte proliferation," and "regulation of inflammatory response." These pathways regulate cytokine secretion, chemotaxis, and thus immune cell infiltration in the TME, while inflammatory factors may promote tumor cell colonization and metastasis.[19] Among them, lipopolysaccharide-induced ReIB and p100 expression, the dependent mechanism of β1 integrin expression, and NF-κB is precisely the ReIB nuclear translocation. The NF-κB signaling pathway is known to play an important role in SCLC carcinogenesis.[20] At the GO-CC level, the robust DEGs were predominantly enriched in "membrane raft," "membrane microdomain," "membrane region," and "external side of the plasma membrane." Chemokines usually regulate the localization and migration of endogenous cells. Similarly, tumor cells use this property for disorderly regulation[19] KEGG analysis revealed that the robust DEGs were enriched in "complement and coagulation cascades," "human T-cell leukemia virus 1 infection," and "ECM-receptor interaction" signaling pathways. The complement system is an important regulatory pathway in the immunosuppressive state of primary tumors and metastatic target organs, and is involved in processes related to inflammatory factors and tumorigenesis. Complement can recruit and induce aggregation of immunosuppressive cells in the TME; furthermore, inhibition of complement expression and blockade of programmed cell death factors have synergistic antitumor effects that retarded tumor progression in mouse models of lung cancer[21]. "Human T-cell leukemia virus 1 infection" is involved in inflammatory factor-related pathways, while the "ECM-receptor interaction" pathway activates second messengers[18].

This study identified six hub genes: *ITGA10*, *DUSP12*, *PTGS2*, *FOS*, *TGFBR2*, and *ICAM1*. Among them, *PTGS2* is an inducible immediate response gene that is negative for most cells in a normal physiological state; however, in pathological responses such as inflammation or tumors, *PTGS2* is affected by certain cytokines, growth factors, inflammatory mediators, pro-oncogenic factors, hypoxia, hormones, etc. Prostaglandins, the main product of the PTGS2 enzyme, have

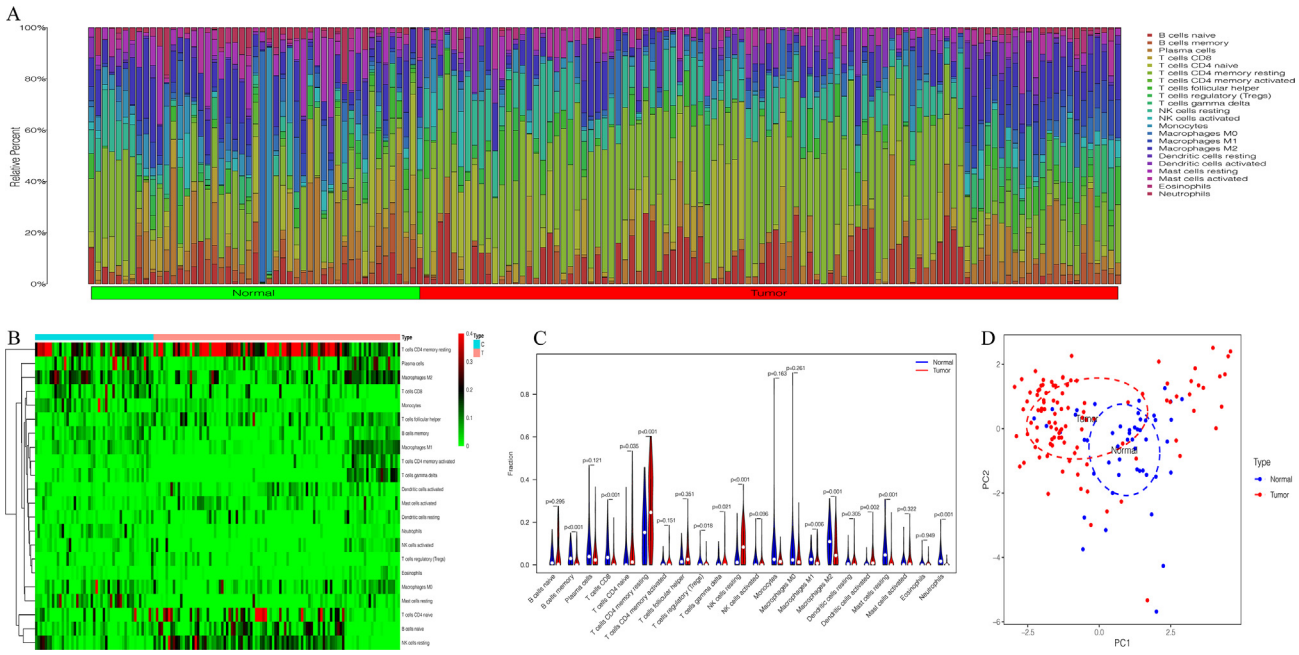

Figure 4. Immune cell infiltration analysis. (A) Distribution of 22 immune cells between SCLC tumor tissue and normal tissue samples. (B,C) The difference in immune cell infiltration between SCLC tumor tissue and normal tissue samples was visualized by heatmap (B) and violin plot (C). (D) PCA plot of 22 immune cells. SCLC tumor samples (red) and normal samples (blue) are plotted along the axis of the first two principal components (PC1 and PC2). PCA: Principal components analysis; SCLC: Small cell lung cancer.

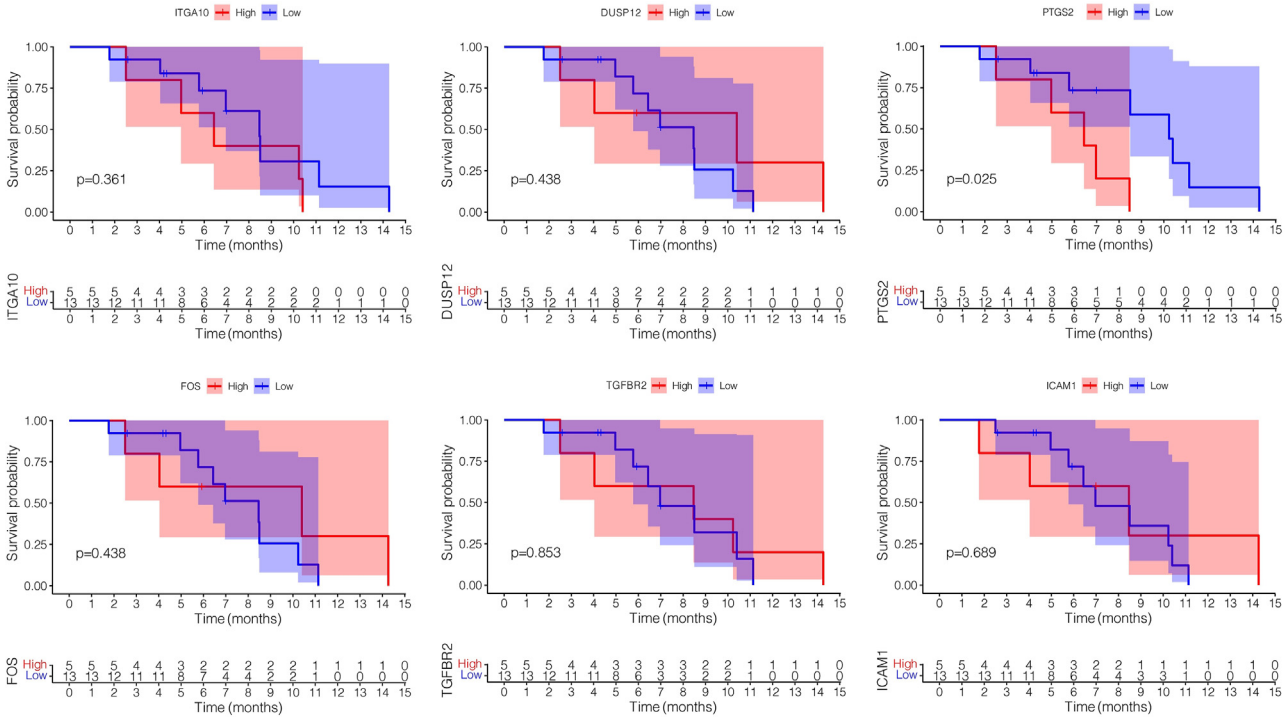

Figure 5. Survival analysis of hub genes.

biological activities such as inhibition of cell death, promotion of cell proliferation, inhibition of immune surveillance, and promotion of angiogenesis. A study[22] has suggested that aspirin, which targets PTGS2, is a potential therapeutic target for patients with SCLC.

The present study also describes the TME landscape and elaborates on the infiltration characteristics of 22 immune cell species in SCLC and normal tissue samples. In addition, the immune cell components associated with SCLC development were identified. There were significant differences between SCLC and normal tissue samples in the infiltration level of memory B cells, $CD8^+$ T cells, resting memory $CD4^+$ T cells, resting NK cells, M1 and M2 macrophages, activated dendritic cells, resting mast cells, and neutrophils. Different components of the TME are

responsible for different clinical outcomes. The immune system prevents cancer development predominantly by recognizing and killing tumor cells through cytotoxic T lymphocytes. However, tumor cells often develop ways to evade immune surveillance, for example, by activating the programmed cell death 1 (PD-1) receptors. Binding between the PD-1 receptor and its ligand PD-L1 or PD-L2 inhibits the function of other cells through inducing non-responsiveness, promoting apoptosis, and reducing proliferation and secretion of inflammatory cytokines such as interferon (IFN) -γ, interleukin 4, and interleukin 2. Therefore, it is important to develop biomarkers that can predict whether immune checkpoint therapies will benefit specific patients with SCLC. In addition, despite the significant differences in immune cell infiltration between SCLC and normal tissue samples, PCA could not completely distinguish between SCLC and normal samples owing to the data batch effect interfering with gene expression.

In combination with previous studies, the six prognosis-related hub genes obtained in the present study may help elucidate the molecular mechanisms of SCLC. However, although the study has indicated potential hub genes and key pathways in SCLC, there are still limitations to the study. First, the gene modules were mined based on the PPI networks in the STRING database, where some proteins were based on predictions rather than molecular experiments. Therefore, the molecular mechanisms of these key pathways and hub genes require further molecular investigation. Second, this study is purely a bioinformatics analysis, and consequently, experimental studies are needed to validate the observations.

Funding

None.

Author contributions

Li Zhang: Conceptualization, methodology, supervision, reviewing and editing; Jun Ni: Methodology, software, data curation, visualization and writing-original draft preparation; Xiaoyan Si: Supervision and editing; Hanping Wang: Supervision and editing; Xiaotong Zhang: Supervision, editing and conceptualization.

Ethics statement

None.

Data availability statement

The datasets used in the current study are available from the corresponding author on reasonable request.

Conflicts of interest

None.

Acknowledgments

None.

Appendix A. Supplementary data

Supplementary data to this article can be found online at https://doi.org/10.1016/j.cpt.2022.09.004.

References

1. Siegel RL, Miller KD, Jemal A. Cancer statistics, 2019. *CA A Cancer J Clin*. 2019;69:7–34. https://doi.org/10.3322/caac.21551.
2. Chen W, Zheng R, Baade PD, et al. Cancer statistics in China, 2015. *CA A Cancer J Clin*. 2016;66:115–132. https://doi.org/10.3322/caac.21338.
3. Silva M, Galeone C, Sverzellati N, et al. Screening with low-dose computed tomography does not improve survival of small cell lung cancer. *J Thorac Oncol*. 2016;11:187–193. https://doi.org/10.1016/j.jtho.2015.10.014.
4. Byers LA, Rudin CM. Small cell lung cancer: where do we go from here? *Cancer*. 2015;121:664–672. https://doi.org/10.1002/cncr.29098.
5. Horn L, Mansfield AS, Szczęsna A, et al. First-line atezolizumab plus chemotherapy in extensive-stage small-cell lung cancer. *N Engl J Med*. 2018;379:2220–2229. https://doi.org/10.1056/NEJMoa1809064.
6. Paz-Ares L, Dvorkin M, Chen Y, et al. Durvalumab plus platinum-etoposide versus platinum-etoposide in first-line treatment of extensive-stage small-cell lung cancer (CASPIAN): a randomised, controlled, open-label, phase 3 trial. *Lancet*. 2019;394:1929–1939. https://doi.org/10.1016/S0140-6736(19)32222-6.
7. George J, Lim JS, Jang SJ, et al. An emerging place for lung cancer genomics in 2013. *J Thorac Dis*. 2013;5:S491–S497. https://doi.org/10.3978/j.issn.2072-1439.2013.10.06.
8. George J, Lim JS, Jang SJ, et al. Comprehensive genomic profiles of small cell lung cancer. *Nature*. 2015;524:47–53. https://doi.org/10.1038/nature14664.
9. Hendriks LEL, Menis J, Reck M. Prospects of targeted and immune therapies in SCLC. *Expert Rev Anticancer Ther*. 2019;19:151–167. https://doi.org/10.1080/14737140.2019.1559057.
10. Bremnes RM, Busund LT, Kilvær TL, et al. The role of tumor-infiltrating lymphocytes in development, progression, and prognosis of non-small cell lung cancer. *J Thorac Oncol*. 2016;11:789–800. https://doi.org/10.1016/j.jtho.2016.01.015.
11. Ott PA, Bang YJ, Piha-Paul SA, et al. T-cell-inflamed gene-expression profile, programmed death ligand 1 expression, and tumor mutational burden predict efficacy in patients treated with pembrolizumab across 20 cancers: keynote-028. *J Clin Oncol*. 2019;37:318–327. https://doi.org/10.1200/JCO.2018.78.2276.
12. Rohrbeck A, Neukirchen J, Rosskopf M, et al. Gene expression profiling for molecular distinction and characterization of laser captured primary lung cancers. *J Transl Med*. 2008;6:69. https://doi.org/10.1186/1479-5876-6-69.
13. Ritchie ME, Phipson B, Wu D, et al. Limma powers differential expression analyses for RNA-sequencing and microarray studies. *Nucleic Acids Res*. 2015;43:e47. https://doi.org/10.1093/nar/gkv007.
14. Kolde R, Laur S, Adler P, et al. Robust rank aggregation for gene list integration and meta-analysis. *Bioinformatics*. 2012;28:573–580. https://doi.org/10.1093/bioinformatics/btr709.
15. Yu G, Wang LG, Han Y, et al. clusterProfiler: an R package for comparing biological themes among gene clusters. *OMICS*. 2012;16:284–287. https://doi.org/10.1089/omi.2011.0118.
16. Chen B, Khodadoust MS, Liu CL, et al. Profiling tumor infiltrating immune cells with CIBERSORT. *Methods Mol Biol*. 2018;1711:243–259. https://doi.org/10.1007/978-1-4939-7493-1_12.
17. Karachaliou N, Pilotto S, Lazzari C, et al. Cellular and molecular biology of small cell lung cancer: an overview. *Transl Lung Cancer Res*. 2016;5:2–15. https://doi.org/10.3978/j.issn.2218-6751.2016.01.02.
18. Sundaresan V, Lin VT, Liang F, et al. Significantly mutated genes and regulatory pathways in SCLC — a meta-analysis. *Cancer Genet*. 2017;216–217:20–28. https://doi.org/10.1016/j.cancergen.2017.05.003.
19. Wu Q, Wang D, Zhang Z, et al. DEFB4A is a potential prognostic biomarker for colorectal cancer. *Oncol Lett*. 2020;20:114. https://doi.org/10.3892/ol.2020.11975.
20. Saito T, Sasaki CY, Rezanka LJ, et al. P52-independent nuclear translocation of RelB promotes LPS-induced attachment. *Biochem Biophys Res Commun*. 2010;391:235–241. https://doi.org/10.1016/j.bbrc.2009.11.039.
21. Taddei ML, Parri M, Mello T, et al. Integrin-mediated cell adhesion and spreading engage different sources of reactive oxygen species. *Antioxidants Redox Signal*. 2007;9:469–481. https://doi.org/10.1089/ars.2006.1392.
22. Gong L, Zhang D, Dong Y, et al. Integrated bioinformatics analysis for identificating the therapeutic targets of aspirin in small cell lung cancer. *J Biomed Inf*. 2018;88:20–28. https://doi.org/10.1016/j.jbi.2018.11.001.